

# Supplementary Material

## Aerosol-Jet Printed Fine-Featured Triboelectric Sensors for Motion Sensing

*Qingshen Jing, Yeon Sik Choi, Michael Smith, Nordin Catic, Canlin Ou, Sohini Kar-Narayan\**

### Note S1

The relationship among maximum detectable velocity, given grating period and sampling rate can be calculated as the following.

$$f_{sampling} = N \cdot f_{max\ signal} = N \cdot \frac{v_{max}}{d_{grating\ period}} \quad (s1)$$

Where  $f_{sampling}$  is the sampling rate determined by the data collecting hardware and the software,  $f_{max\ signal}$  is the maximum signal frequency the set up can detect, which results from dividing maximum detectable velocity ( $v_{max}$ ) by grating period ( $d_{grating\ period}$ ). 'N' is the factor to ensure enough sampling points in each cycle being collected to reproduce the actual signal curve. N=10 can be an acceptable factor if the shape of the signal is considered to be important. Thus, with voltmeter having a sampling rate of 10 kHz, a motion sensor with 50  $\mu$ m period width is capable to detect velocity up to 50 mm/s. And if maximum velocity detecting required goes up to 5 m/s with the same data collection set up, the grating period should be designed at least 5 mm accordingly. To increase the sampling rate can increase the maximum detectable velocity for a fixed grating period, however may bring in unnecessary cost for hardware and software upgrade.

## **Note S2**

The acquisition and processing of the signals generated from the 3-channeled rotary sensor is explained in detail here.

Analog voltage signals from the circuit shown in Figure 4a were monitored continuously and were compared with a triggering threshold value which was set being positive and slightly higher than the positive noise level when the sensor was static. Once the voltage signal was higher than the triggering threshold, the program would treat the signal as generating a positive pulse, followed with setting a mark and recording the sequence for this channel. There was also a resetting threshold which was set being negative and slightly lower than the negative noise level when the sensor was static. Once the voltage signal fell below the resetting threshold, the program would treat the signal as being finished with a positive pulse, followed with resetting the mark for this channel. The benefit of such processing method is to ignore the possible differences of signal amplitudes at their peaks due to different sliding velocities, as sometimes the peak value could even exceed the voltage measuring range of the MCU.

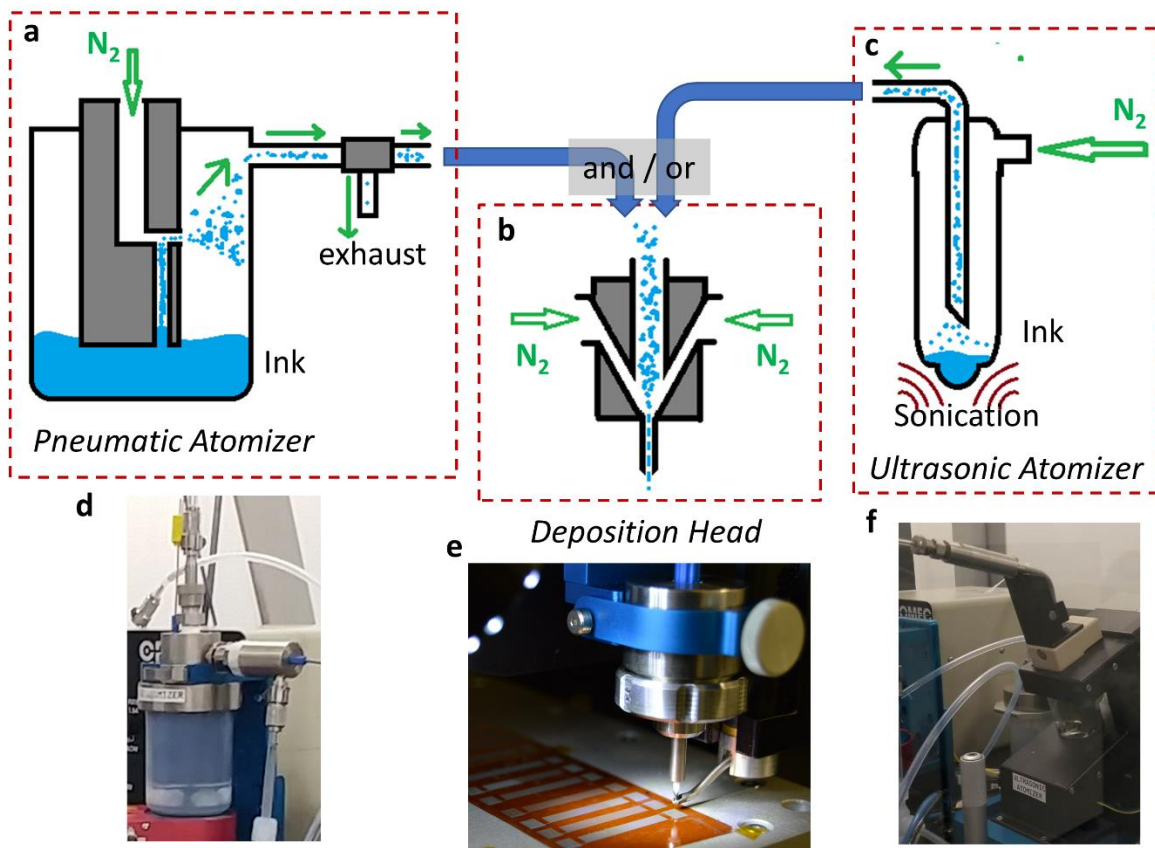


**Figure S1.** The schematic and actual parts of an aerosol jet printer. a) shows ink in a pneumatic atomizer being excited into an aerosol by  $N_2$  air flow followed with compressing and being carried toward the deposition head. b) shows the ink mist being focused by a sheath flow of  $N_2$  and ejected from the deposition head onto a substrate. c) shows ink in an ultrasonic atomizer being excited by sonication and carried toward the deposition head by  $N_2$  air flow. d) ~ f) are photos of actual parts from the printer for the pneumatic atomizer, the deposition head, and the ultrasonic atomizer.

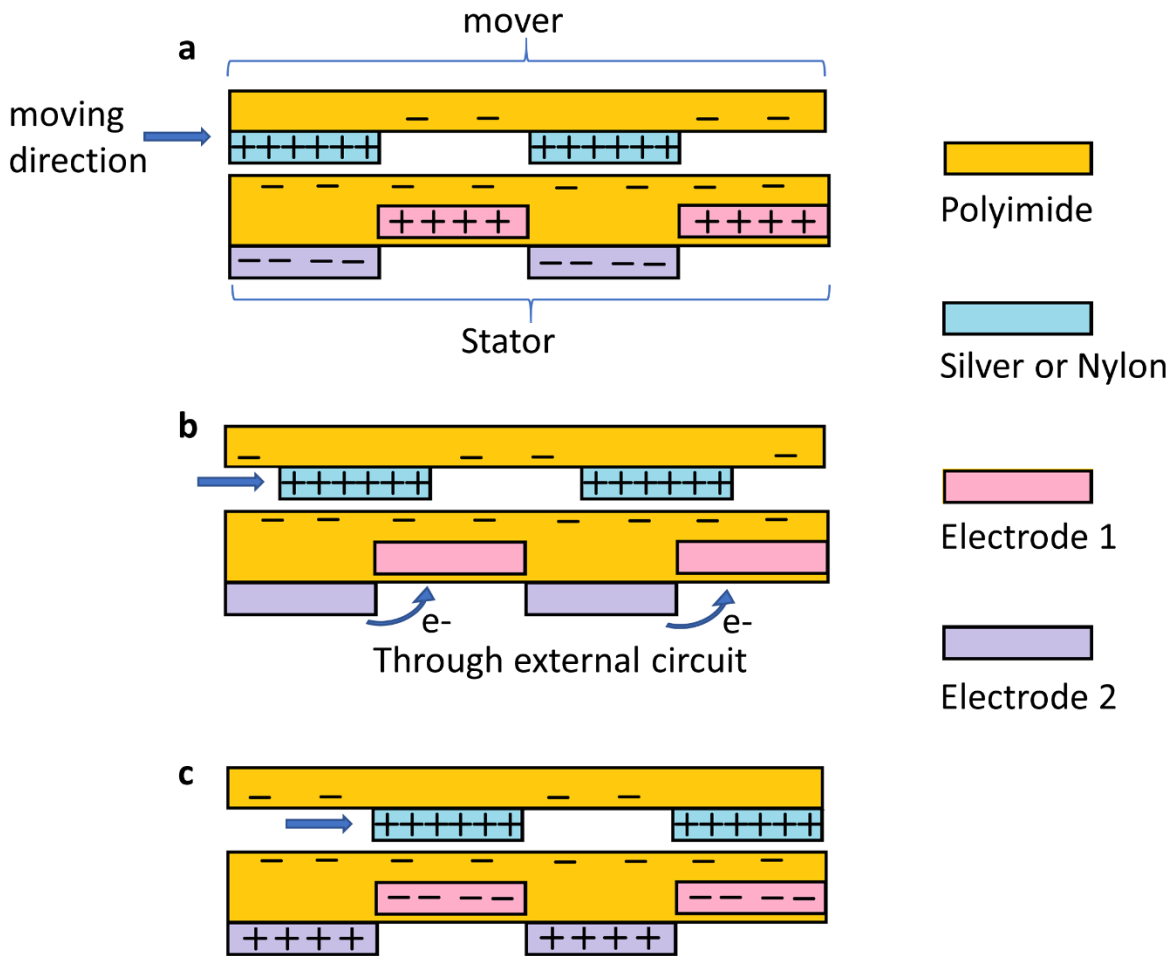


**Figure S2.** Schematic diagram showing the working mechanism of the “free-standing” type of triboelectric sensor. The printed grated mover is sliding over a Kapton film, on the backside of which is a pair of interdigitated electrodes fabricated with our AJP technology mentioned in Figure 1e. a) shows when the silver or the Nylon gratings come into contact with Kapton in the stator, electrons are transferred to and distributed on the surface of Kapton. The unbalanced charge will induce electrons distributed accordingly on the interdigitated electrodes. b) and c) shows when the silver or the Nylon gratings are sliding with the mover at half of a cycle, the electrons flow via external path from one set of the electrodes to another, due to the change of the electric field caused by the movement of the charges on the surface of the silver/Nylon gratings.

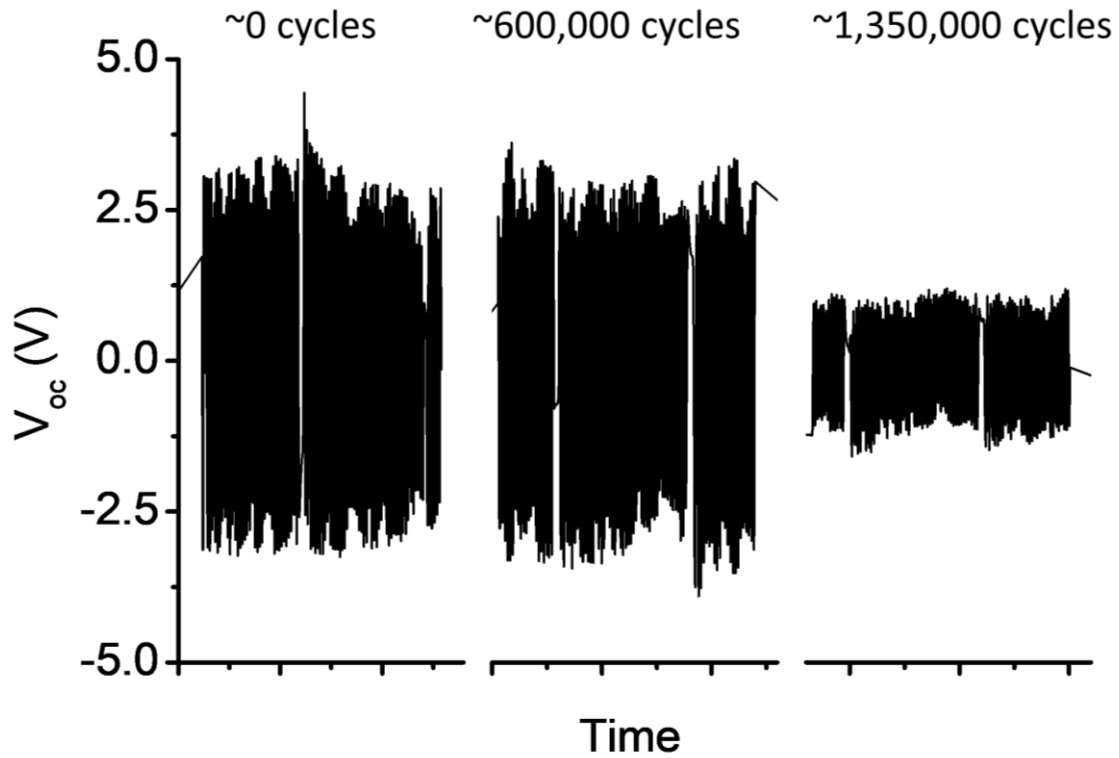


**Figure S3.** Fatigue test of output signals on printed sensors with continuous sliding motion between mover and stator: We conducted a fatigue test with our sliding mode sensor under continuous reciprocating motion. The sample we used had a silver grating period of 600  $\mu\text{m}$ . The stroke for the reciprocating motion was 30 mm. For the first 6,000 rounds of reciprocating sliding (equivalent sliding distance is about 360 m, corresponding to about 600,000 signal cycles), the amplitude of the output signal did not show any obvious difference. However, after about 13,500 rounds of reciprocating sliding (equivalent sliding distance is about 810 m, corresponding to about 1,350,000 signal cycles), the amplitude reduced to half of what was obtained in the first 6,000 rounds. Although the amplitude decreased, the signal kept its original form, which meant it was still possible to generate accurate information for sensing purpose. Periodic cleaning of the contacting surface using ethanol or acetone could recover some of the output. Also, a smaller contacting force can further improve the fatigue performance of the sensor. Moreover, since it is only the materials from the mover that are potentially degraded during the rubbing process (as electrodes on the stator are on the backside and thus protected by the substrate), it is easy to replace the mover with a new one when the performance starts to degrade after thousands of cycles.

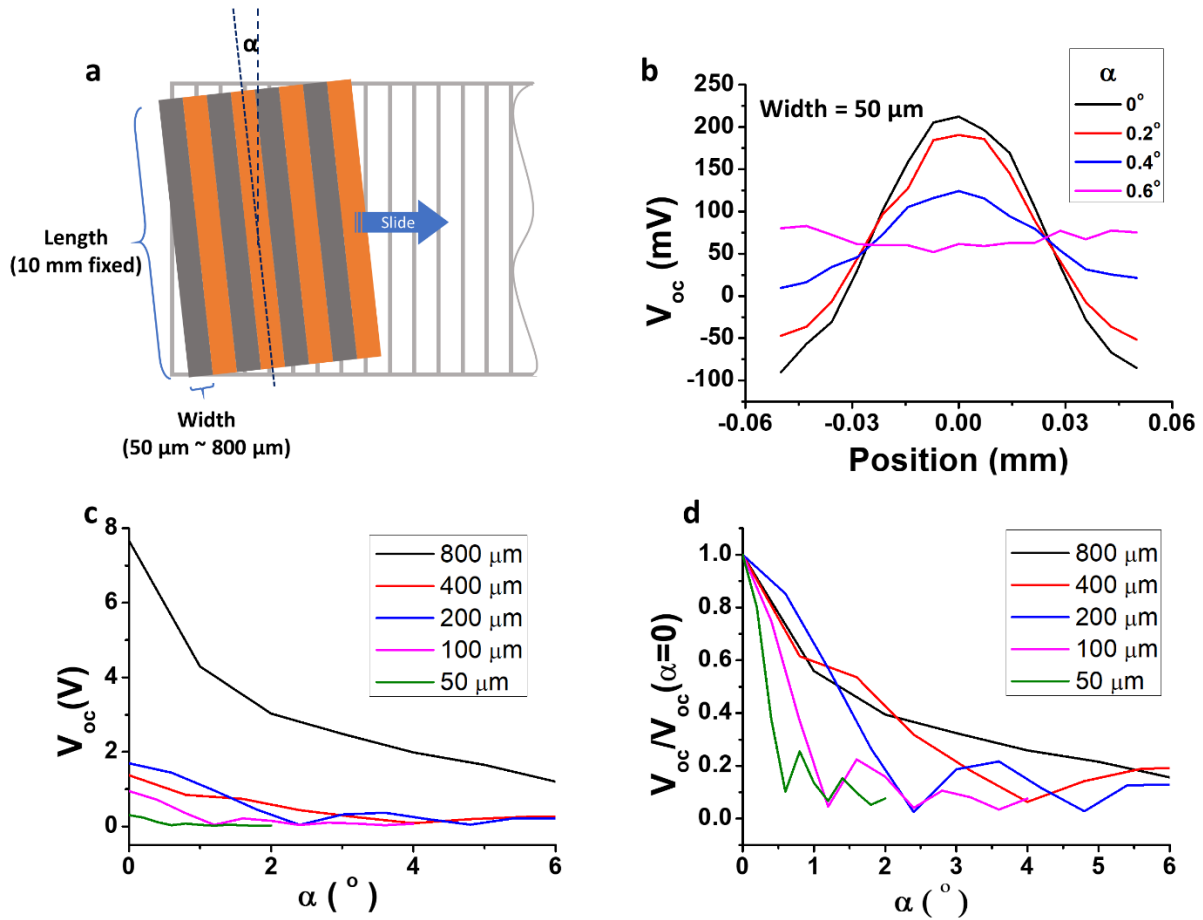


**Figure S4.** Simulation results on angular mismatched sliding. a) illustrates a sliding when the mover has an angular mismatch against the stator. In the simulation, each grating strip is set to have a length of 10 mm, and a width varied from 800 μm to 50 μm. The mismatch angle is marked as  $\alpha$ . Open-circuit voltages are calculated over a full cycle of sliding. b) shows a simulated signal at a strip width of 50 μm with  $\alpha$  varied from 0° to 0.6°. A small angular mismatch could result in a dramatic output drop. c) compared the maximum  $V_{oc}$  with different strip width at different mismatching angles. A wider strip triboelectric generator can tolerant relatively larger angular mismatch compared with a narrower strip triboelectric generator. d) converts the data from c) by normalizing each  $V_{oc}$  with its value from no angular mismatch results ( $\alpha=0^\circ$ ), respectively.

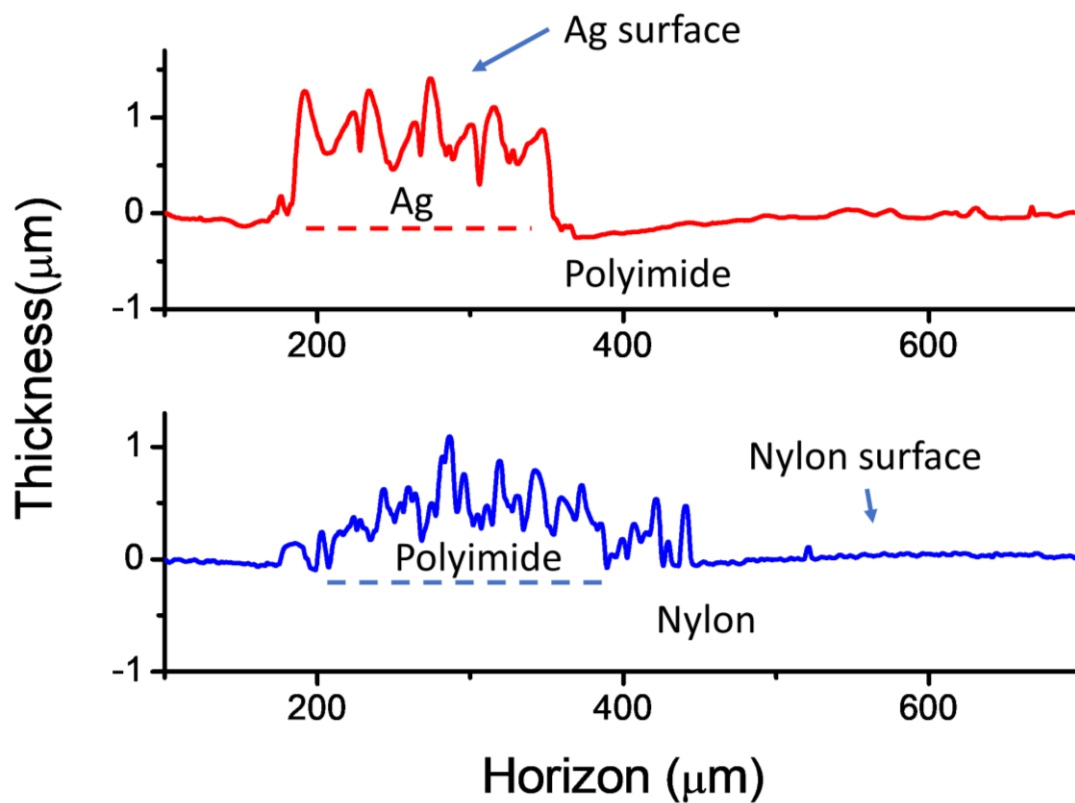


**Figure S5.** A pair of profilometer (Dektak) data showing the surface roughness of the surface of printed Ag and the Nylon film. The top profile shows the cross-section of one printed silver grating on top of the polyimide (PI/Kapton) film. The surface of silver is uneven. The bottom profile shows the cross-section of a printed PI grating on top of Nylon, where in comparison, the surface of Nylon is much smoother than the silver.

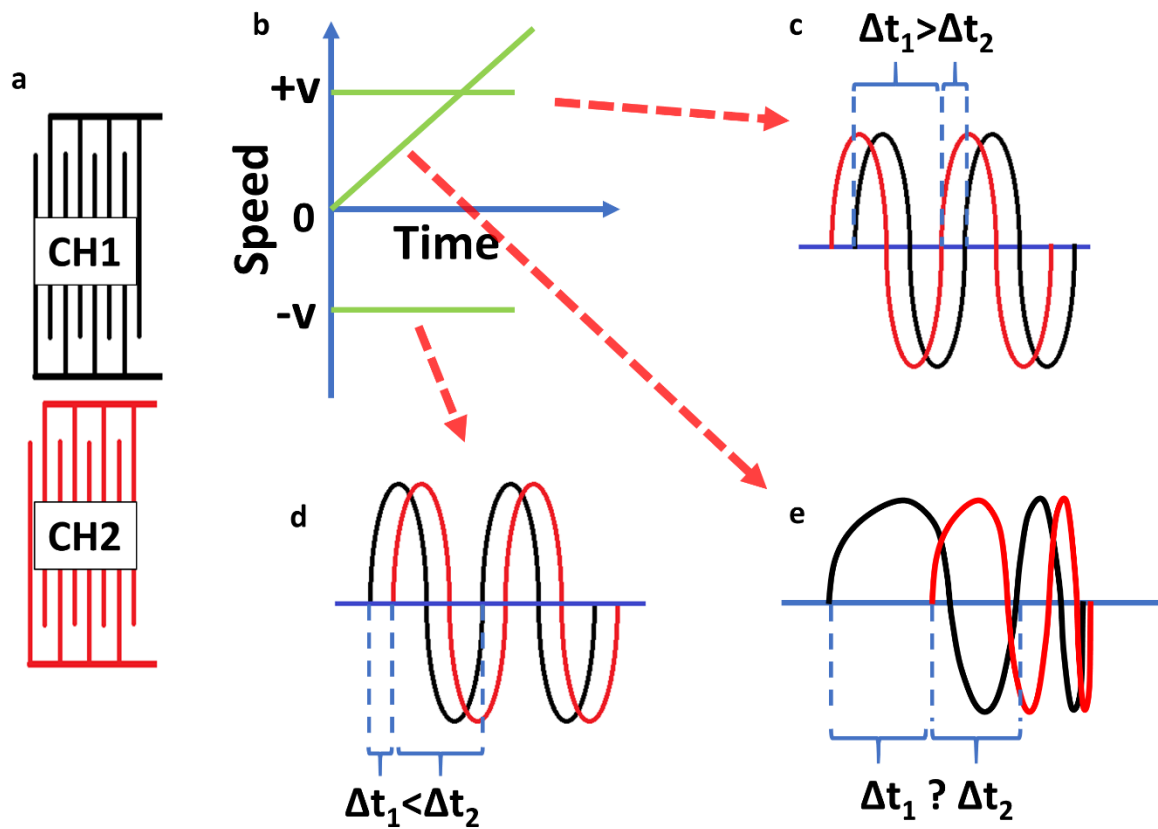


**Figure S6.** The working principle and shortage of the double-channelled triboelectric motion sensor (Ref. Q. Jing, Y. Xie, G. Zhu, R. P. S. Han, Z. L. Wang, Nat. Commun. 2015, DOI 10.1038/ncomms9031.) There is a 1/4 space period difference between channel 1 and channel 2, which results in a signal lag between the two channels when the sensor is operating. The direction of uniform motion can be told by timing and comparing the lag difference of  $\Delta t_1$  and  $\Delta t_2$ , as shown in (c) and (d). However, in a situation of acceleration in (e), the usual comparison between measured time lag could be misleading and resulting in the wrong judgement of motion direction.



<b>Property</b>	<b>Unit</b>	<b>Value</b>	<b>Test method according to</b>
Hardness	Shore A	37	DIN 53505
Density	g/cm <sup>3</sup>	1.18	DIN EN ISO 1183-1-A
Tensile strength	MPa	12	DIN 53504-S2
Elongation at break	%	1150	DIN 53504-S2
Tear strength	N/mm	27	DIN ISO 34-1Bb
Abrasion loss	mm <sup>3</sup>	165	DIN ISO 4649-A

**Table S1.** Property Sheet for Polyurethane (Elastollan® Soft 35 A 12 P)

(Data acquired from BASF, <http://www.tpucl.com/wp-content/uploads/2017/08/Soft-35-A-12P.pdf>)

## **Movie M1**

A movie is provided showing an all-printed 3-channeled rotary sensor working at real time. The sensor's stator was made from silver printed on Kapton film, and the mover (rotator) was made from polyimide printed on Nylon film. We used a piece of sponge and a plastic handle to achieve conformal contact and better control between the mover and the stator.